



# Microstructural, magnetic and mechanical property changes in an AISI 444 stainless steel aged in the 560 °C to 800 °C range

S.S.M. Tavares<sup>a,\*</sup>, J.A. de Souza<sup>a</sup>, L.F.G. Herculano<sup>b</sup>, H.F.G. de Abreu<sup>b</sup>, C.M. de Souza Jr.<sup>c</sup>

<sup>a</sup>Universidade Federal Fluminense, Departamento de Engenharia Mecânica/PGMEC, Rua Passo da Pátria, 156, CEP 24210-240, Niterói/RJ, Brazil

<sup>b</sup>Universidade Federal do Ceará, Departamento de Engenharia Metalúrgica, Brazil

<sup>c</sup>Universidade Federal do Rio de Janeiro, Departamento de Engenharia Metalúrgica e de Materiais, Brazil

## ARTICLE DATA

### Article history:

Received 4 October 2006

Received in revised form

4 November 2006

Accepted 7 November 2006

### Keywords:

Ferritic stainless steel

Aging

AISI 444

## ABSTRACT

AISI 444 steel is an 18Cr–2Mo ferritic stainless steel, containing Ti and Nb as stabilizing elements. The effects of aging in the 560–800 °C range on the microstructure, mechanical and magnetic properties were investigated. The material was not susceptible to sigma phase formation until 100 h of exposure. Slight hardening at 560 °C and progressive softening in the 650 °C–800 °C range were observed. At these temperatures, Mo-rich phases such as Fe<sub>2</sub>Mo and FeMoSi precipitate. The increase of particle sizes with the increase of temperature above 650 °C is responsible for the decrease of hardness. Precipitation of the Mo-rich phases increases the coercive force.

© 2006 Elsevier Inc. All rights reserved.

## 1. Introduction

Ferritic stainless steels are widely used in many manufacturing processes in chemical and petrochemical industries. The main advantage of this steel family over the austenitic grades (304, 316,...) is the superior stress corrosion resistance in certain of these environments. However, ferritic stainless steels are susceptible to some embrittlement phenomena related to grain growth, sigma phase formation [1,2] and  $\alpha'$  precipitation [2,3].

AISI 444 is a ferritic type stainless steel containing 18% Cr, 2% Mo and Ti and/or Nb as stabilizing elements. Due to the Cr and Mo contents the steel presents higher pitting corrosion resistance than other ferritic grades. The Ti and/or Nb stabilizing elements form fine carbides which prevent sensitization and improve the weldability. In previous work of our group [4], the effects of low temperature prolonged aging (400–475 °C) were investigated. At these temperatures the steel undergoes hardening, embrittlement and corrosion resistance decay, due to  $\alpha'$  precipitation.

The aim of the present work was to investigate the microstructural changes in the AISI 444 exposed to temperatures in the 560 °C–800 °C range. The effects of the precipitation reactions on the mechanical properties (hardness and toughness) and magnetic properties (coercive force and magnetization saturation) were determined.

## 2. Experimental Methods

The 3 mm thick plate of AISI 444 studied in this work was purchased in the annealed condition. Table 1 shows the chemical composition of the material.

**Table 1 – Chemical composition of the AISI 444 studied**

% C	% Cr	% Ni	% Mo	% Ti	% Nb	% Si	% N	% Fe
0.015	17.56	0.20	1.86	0.13	0.18	0.54	0.0123	Bal.

\* Corresponding author. Tel.: +55 21 26295584.

E-mail address: [ssmtavares@terra.com.br](mailto:ssmtavares@terra.com.br) (S.S.M. Tavares).

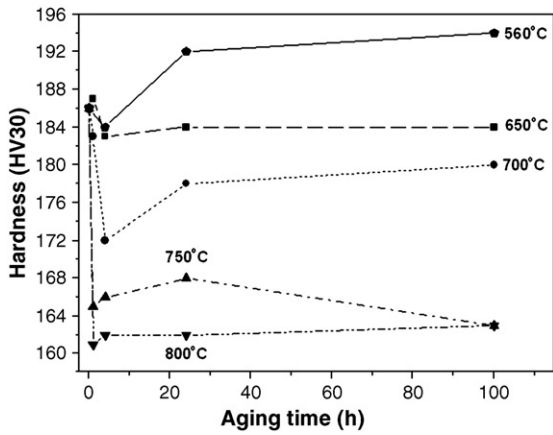


Fig. 1–Hardness × aging time at 560 °C, 650 °C, 700 °C, 750 °C and 800 °C.

AISI 444 steel is strongly notch sensitive. Using Charpy-V notch reduced size samples (55×10×2.5 mm) very small absorbed energy values were found to cause fracture in the received condition: 3 J. On the other hand, using an unnotched sample the fracture energy was raised to 120 J. For this reason, unnotched specimens were used to evaluate the effects of aging on the toughness. The tests were conducted in a universal impact test machine with maximum capacity of 300 J and a precision of ±1 J. Vickers hardness (HV30) was measured in all conditions.

The samples were treated at 560 °C, 650 °C, 700 °C, 750 °C and 800 °C for various times up to 100 h.

Microstructural changes were investigated by optical and scanning electron microscopy and X-ray diffraction. Samples for optical and scanning electron microscopy were prepared with Vilella’s reagent [5]. Precipitates were extracted from the samples aged at 700 °C and 750 °C for 24 h. The precipitation extraction was made in a 10% HCl solution applying a current density of 0.25 A/cm<sup>2</sup>. The precipitates were analyzed by EDS and X-ray diffraction.

Saturation magnetization and coercive force changes were measured using a Vibrating Sample Magnetometer with

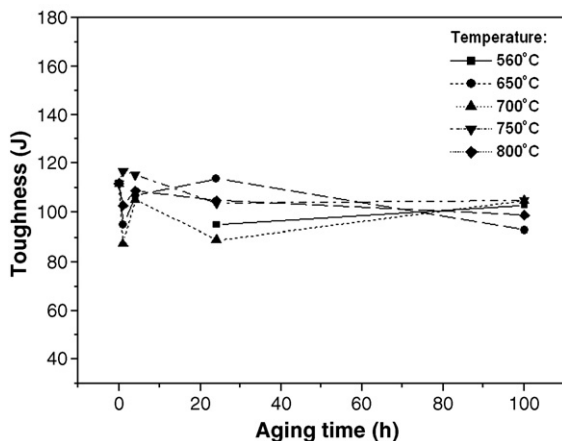


Fig. 2–Impact energy × aging time at 560 °C, 650 °C, 700 °C, 750 °C and 800 °C.

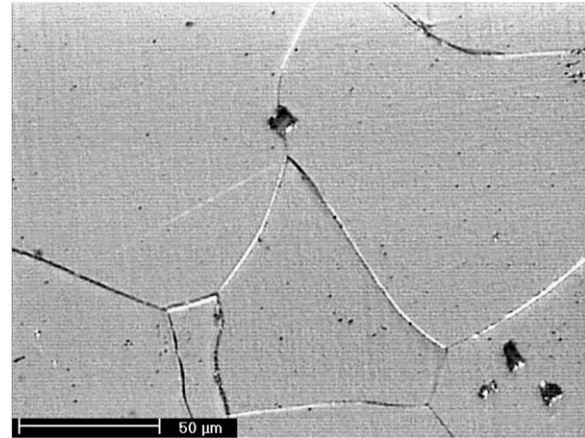


Fig. 3–Microstructure of the as received material.

maximum applied field of 1T, and a time constant and sweep time of 1 ms and 30 min, respectively.

### 3. Results and Discussion

Fig. 1 shows the hardness variation with aging time at five different temperatures. Fig. 2 shows the impact toughness versus aging time for the same temperatures. The aging at 560 °C slightly increases the hardness, whereas aging at 650 °C showed essentially no hardness change. Increasing the aging temperature to 700 °C, 750 °C and 800 °C promotes progressive softening of the material. Fig. 2 shows that the material did not present any embrittlement effect in the temperatures investigated for times up to 100 h.

Some ferritic stainless steels are susceptible to sigma phase formation in the 500–800 °C range; this causes hardening and embrittlement. Sigma phase precipitation is favoured by an increase in Cr, Mo and Si contents. One of the objectives of this work was to investigate the susceptibility of the AISI 444 steel to sigma phase formation. The hardness and toughness results presented in Figs. 1 and 2 indicate that the hard and brittle sigma phase does not form for the aging conditions investigated.

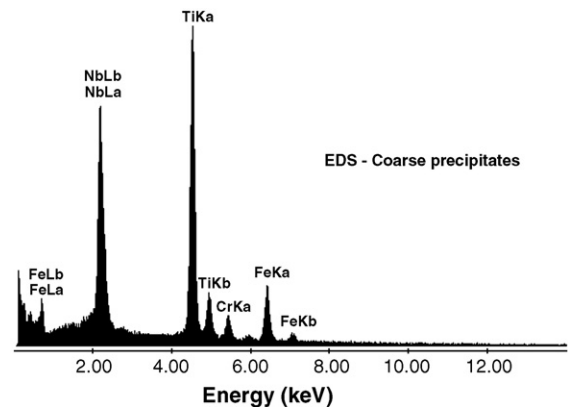


Fig. 4–EDS profile of the coarse square shaped precipitates in the as received condition.

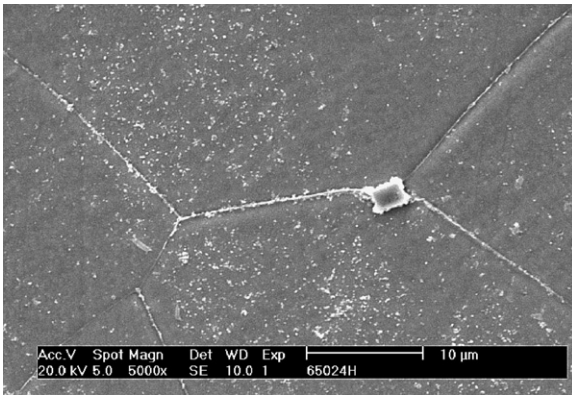


Fig. 5 – Microstructure of the sample aged at 650 °C for 24 h.

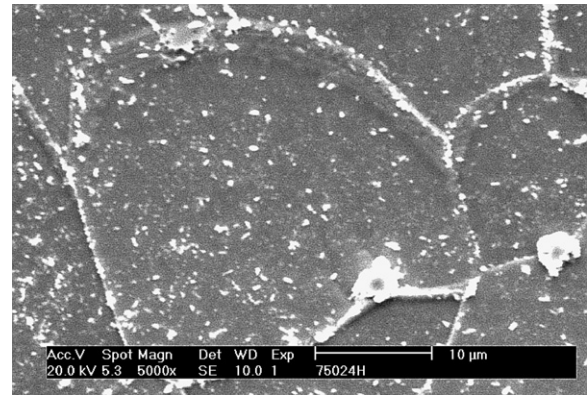


Fig. 7 – Microstructure of the sample aged at 750 °C for 24 h.

The starting material presents a microstructure containing coarse and square shaped precipitates in the ferritic matrix (Fig. 3). These are Ti and Nb nitrides, as confirmed by EDS analysis (Fig. 4). Figs. 5, 6, 7, and 8 show SEM images of the microstructures of the samples aged for 24 h at 650 °C, 700 °C, 750 °C and 800 °C, respectively, all revealed by Vilella's etch. These microstructures indicate the original (Nb,Ti)N precipitates and other fine and dispersed particles precipitated in the ferritic matrix. The average size of the new precipitates increases with the aging temperature; this coarsening is related to the hardness decrease with the increase of aging temperature.

Fig. 9 shows EDS results for the powder extracted from the sample aged at 700 °C for 24 h. The sample aged at 750 °C showed a similar profile (not shown). The precipitates exhibit high Si, Mo and Ti contents. Niobium may also be present, but its presence may be obscured since its strongest peaks occur at the same energy level as the Mo (L transition). The low Cr content confirms the absence of  $\sigma$  phase.

The X-ray diffractograms of the powders extracted from samples aged at 700 °C and 750 °C are shown in Figs. 10 and 11, respectively. Using the JCPDS data base [6], the peaks were related to reflections of the phases  $\text{Fe}_2\text{Mo}$  (JCPDS 43-0822),  $\text{Fe}_7\text{Mo}_3$  (JCPDS 45-1230),  $\text{Fe}_{63}\text{Mo}_{37}$  (JCPDS 19-0608), and niobium and titanium nitrides (JCPDS 43-1421, 14-0547, 74-1214 and 17-0386). Many coincidences were also found with the FeMoSi phase (JCPDS 15-0485), which is in accordance to the EDS

result, which shows a significant peak for Si. There is some question as to whether this is a ternary phase or if there exists a continuous solid solution between  $\text{Fe}_2\text{Mo}$  and FeSiMo, with the Si replacing Fe atoms (see card JCPDS 15-0485 of [6]).

The Fe–Mo and Fe–Mo–Si phases are those which precipitate during the high temperature aging, especially  $\text{Fe}_2\text{Mo}$  and FeMoSi which present a significant number of peaks coincident with the diffractogram obtained. Some peaks of the X-ray diffractogram, however, were identified as iron–molybdenum oxides (JCPDS 35-1479 and 15-0290), which probably form due to the extraction and separation process. Ultra-fine niobium and titanium carbides, which are probably present in the stabilized steel, were not detected by the X-ray diffraction of the extracted powder.

Previous work has shown that  $\text{Fe}_2\text{Mo}$  particles are responsible for mechanical and magnetic hardening in Fe–Mo–Ni alloys [7–9]. Jin et al. [10] have also observed mechanical and magnetic hardening of Fe–Cr–Mo alloys with 11 to 17% Cr and 4 to 6% Mo. In these alloys, a significant increase of the coercive force was observed when the alloys were cold deformed and aged in the 615–705 °C range.

Fig. 12 shows the effects of aging in the 560–800 °C range on the coercive force ( $H_c$ ) and saturation magnetization ( $m_s$ ) of the AISI 444 steel. The samples were aged for 24 h. The results were normalized by dividing the  $H_c$  and  $m_s$  values by those of the as received material ( $H_{c(0)}$  and  $m_{s(0)}$ ). It is interesting to note that the saturation magnetization ( $m_s$ ) is not affected by

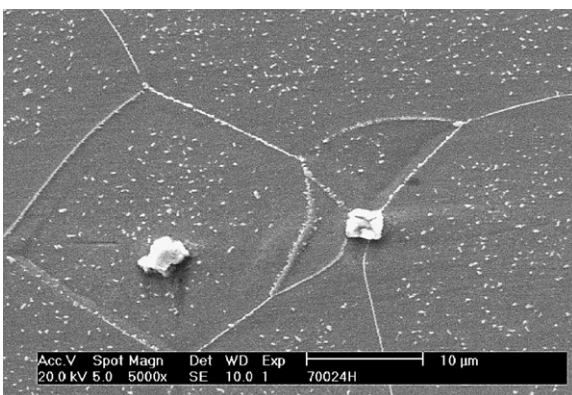


Fig. 6 – Microstructure of the sample aged at 700 °C for 24 h.

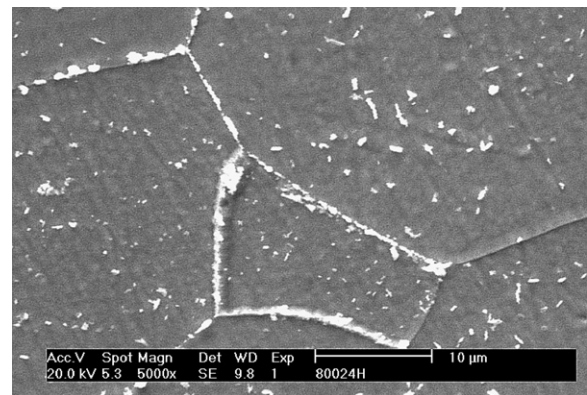


Fig. 8 – Microstructure of the sample aged at 800 °C for 24 h.

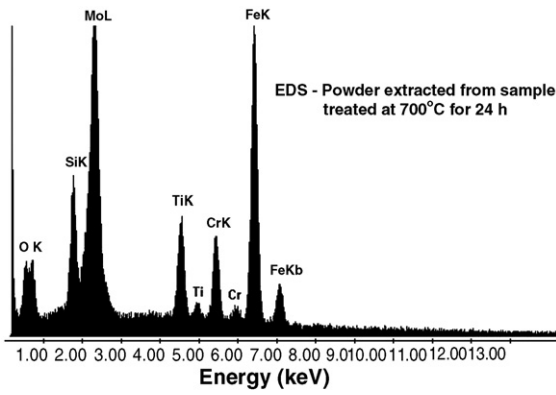


Fig. 9 – EDS profile of the powder extracted from the sample aged at 700 °C for 24 h.

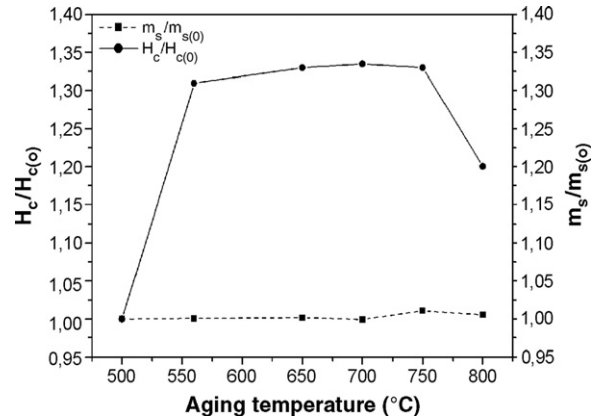


Fig. 12 – Curves of coercive force and saturation magnetization against aging temperature, for samples aged for 24 h.

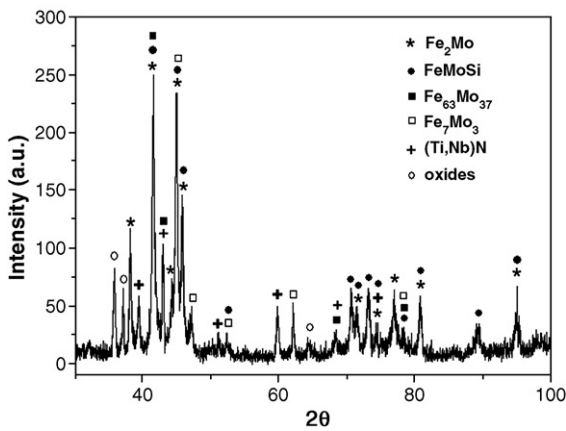


Fig. 10 – X-ray diffraction of samples aged at 700 °C for 24 h.

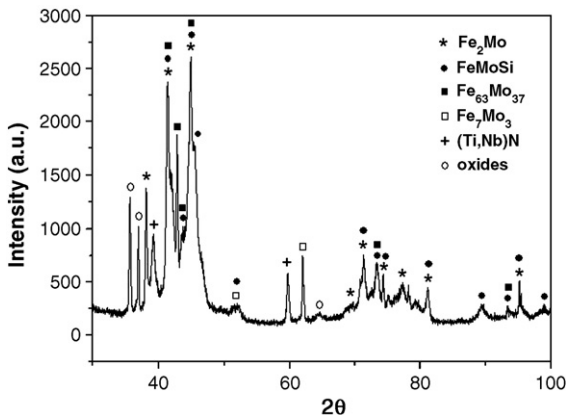


Fig. 11 – X-ray diffraction of samples aged at 750 °C for 24 h.

the precipitation reactions. On the other hand, the material exhibits a magnetic hardening effect, due to the precipitation of Fe–Mo phases. An increase of about 30% in the coercive force is observed. This effect can be enhanced by an increase of the Mo content and by cold deformation before aging, as pointed out by Jin et al. [10].

#### 4. Conclusions

AISI 444 ferritic steel aged in the 560 °C–800 °C range for times up to 100 h did not present sigma phase formation. Aging at 560 °C promotes a small hardening effect, due to the small size of intergranular precipitates that develop. Based on X-ray diffraction analyses, these precipitates are Fe–Mo phases such as Fe<sub>2</sub>Mo, Fe<sub>7</sub>Mo and Fe<sub>63</sub>Mo<sub>37</sub> and are seen to precipitate copiously at 700 and 750 °C. As the aging temperature is increased, progressive softening is observed, reflecting an increase of the precipitate particle size.

Aging in the 560 °C–800 °C does not affect the room temperature toughness of the material, which indicates that the Fe–Mo phases are not harmful to this property.

The precipitation of Fe–Mo phases also promotes a small magnetic hardening effect, especially in the 560 °C–750 °C range, but has no effect on the saturation magnetization.

#### Acknowledgements

The authors are grateful to the Brazilian research agencies (CAPES, FAPERJ and CNPq) for financial support, and also to Dr. Tarcísio R. Oliveira for fruitful discussion.

#### REFERENCES

- [1] Davis JR, editor. ASM speciality handbook—stainless steel. Materials Park, Ohio: ASM (American Society for Materials); 1994.
- [2] Van Zwieten ACTM, Bulloch JH. Some considerations on the toughness properties of ferritic stainless steels — a brief revision. Int J Press Vessels Piping 1993;56:1–31.

- 
- [3] Grobner PJ. The 885 °F (475 °C) embrittlement of ferritic stainless steels. *Metall Trans* 1973;4:251–60.
- [4] de Souza JA, Abreu HFG, Lima Neto P, Tavares SSM, Nascimento AM, de Paiva JAC. Effects of low temperature aging on the AISI 444 steel. *J Mater Eng Perform* 2005; 14(3):367–72.
- [5] Vander Voort GF. *Metallography—principles and practices*. Ohio: ASM International; 1999.
- [6] JCPDS data basis. Newtown Square-PA/USA: International Centre for Diffraction Data; 2000.
- [7] Jin S, Tiefel TH. New ductile Fe–Mo–Ni alloys. *J Appl Phys* 1981;52(3):2503–4.
- [8] Tavares SSM, Teodósio JR, Neto JM. Magnetic hardening in a hot rolled Fe–20Mo–5Ni–0.12C alloy. *J Magn Magn Mater* 1999;182(1–2):193–8.
- [9] Tavares SM, Teodósio JR, Neto JM, da Silva MR. Magnetic properties and thermomagnetic analysis of a Fe–20Mo–5Ni–0.075C alloy. *J Mater Sci* 1999;34:4545–9.
- [10] Jin S, Bennett JE, Archer WE. New Fe–Cr–Mo glass-sealable semi-hard magnet alloys for remanent reed contacts. *IEEE Trans Magn* 1982;18(6):1454–6.